Design of a self-leveling cam mechanism for a stair climbing wheelchair

Design of a Self-Leveling Cam Mechanism for a Stair Climbing Wheelchair

Quaglia Giuseppe
Politecnico di Torino, Department of Mechanics,
Corso Duca degli Abruzzi 24, 10129, Turin, Italy

Nisi Matteo
Politecnico di Torino, Department of Mechanics,
Corso Duca degli Abruzzi 24, 10129, Turin, Italy

Abstract

This paper presents a new version of *Wheelchair.q*, a wheelchair with stair climbing ability. The wheelchair is able to climb single obstacles or staircases thanks to a hybrid wheel-leg locomotion unit with a triple-wheels cluster architecture. The new concept presented in this work represents an improvement respect to previous versions. Through a different arrangement of functional elements, the wheelchair performances in terms of stability and regularity during movement on stair have been increased. In particular, attention has been paid to ensure a regular and comfortable motion for the user during stair climbing operation. For this reason, a cam mechanism has been introduced and designed with the aim to compensate the oscillation generated on the wheelchair frame by the locomotion unit rotation. A design methodology for the cam profile is presented. Moreover, a parametric analysis on the cam profile and on the mechanism dimensions has been conducted with the aim to find a cam profile with suitable dimensions and performances in terms of pressure angle and radius of curvature.

Keywords: Stair-climbing wheelchair, triple-wheels, cam mechanism, mechanism design, architectural barriers.

1. Introduction

Nowadays, architectural barriers represent an unsolved problem for disable or people with reduced mobility. According to [1] there are around 1.2 million wheelchair users in the UK, roughly 2% of UK population. As regard U.S.A. population, about 3.3 million people (1.4%) use a wheelchair or similar devices and 10.2 million (4.4 %) use a cane, crutches, or walker [2]. Only 28% of wheelchair users are under 60. Disability is strongly related to age: 2.1% of 16-19 year olds; 31% of 50-59 years; 78% of people aged 85 or over [1]. This means that the number of wheelchair users will increase according to the aging society, thus the architectural barriers problem will become even more important. Moreover, the most common barriers to access buildings for adults with impairments are related to physical obstacles [3]. From these data, it is evident that providing autonomy to disabled people is an unsolved challenge.

Problems related to architectural barriers can be faced in two ways. From one side, governments try to introduce standards in order to remove architectural barriers from buildings. From the other side, disable people can be provided with devices able to climb obstacles when architectural barriers cannot be removed for technical or economic reasons.

Some commercial stair-climbing devices already exist but most of them are complex, bulky, heavy, expensive and/or they require a great number of sensors and actuators. Thus, in the research field, several architectures have been proposed with the aim of improving the performances of existing stair-climbing wheelchairs in terms of efficiency, simplicity and stair climbing effectiveness. Stair-climbing mechanisms for wheelchair can be classified according to [4] in the same way as obstacle climbing mobile robots: wheel, leg, track and their hybrid combinations.

In [5] a purely legged wheelchair has been proposed. This solution is very effective for stair-climbing but it has a high control complexity. In [6] and [7] a hybrid wheel-track solution is presented. Through a deformable track, the wheelchair can be adapted for flat ground or for stair-climbing motion. The track guarantees the stability and the regularity during stair-climbing, however, the efficiency is low. By adding a motorized wheel locomotion system for flat ground motion the wheelchair efficiency rises but also the complexity of the structure increases especially due to the necessity of a double motorization.

One of the most common architecture in research works is represented by wheelchairs using a leg-wheel locomotion. This solution combines the high efficiency of wheel on flat ground with the high effectiveness of legged locomotion on stairs as in [8], [9] and [10]. Other interesting solutions are [11] and [12] which present a wheelchair able to climb obstacles through an articulated frame. One of the most interesting solution among leg-wheel locomotion wheelchairs is the one presented in several papers such as [13 - 17]. The prototype proposed in these papers allows each wheel to climb steps thanks to an articulated mechanism. Even if the solution is effective, it requires a high number of motors and a complex control strategy.

Finally, another typology of locomotion system is represented by wheel clusters. In [18] and [19], a two-wheels cluster mechanism is presented. This architecture is not statically stable but should be balanced through a stability controller based on an inverse pendulum model. The high control requirements necessary to maintain the dynamic stability and safety issues are the main drawbacks of this kind of solution. In [20] and [21] a two-wheels cluster solution is presented. In these cases, the static stability is guaranteed by the introduction of additional articulated mechanisms. Finally, [22] presents a triple-wheels cluster solution with a hybrid wheel-track architecture. The wheel cluster is the locomotion unit and ensure the climbing ability while the tracks allow the wheelchair static stability.

Also authors have worked on triple-wheels locomotion systems. In [23], [24] and [25] applications of a wheel cluster system on mobile robots with step climbing ability are presented. The same locomotion unit structure has been proposed also for application on a stair-climbing wheelchair: *Wheelchair.q*. Four versions have already been designed. In [26] and [27], a first approach toward the problem is proposed. The rear triple-wheels locomotion units are coupled with two front idle triple-wheels cluster units. This second units are necessary only for static stability. A third version is presented in [28]. The front triple-wheels units have been replaced with an idle track with the aim to generate a more regular motion for the wheelchair during stair climbing.

Finally, in [29] a fourth developed version is presented and it is showed in Figure 1. This architecture represents an evolution with respect to earlier concepts as regard dimensions, control and structure simplicity, but it is still affected by unsolved issues concerning the static stability and the seat oscillation during stair-climbing. In Figure 1 the free-body diagram of the wheelchair on stairs is represented.

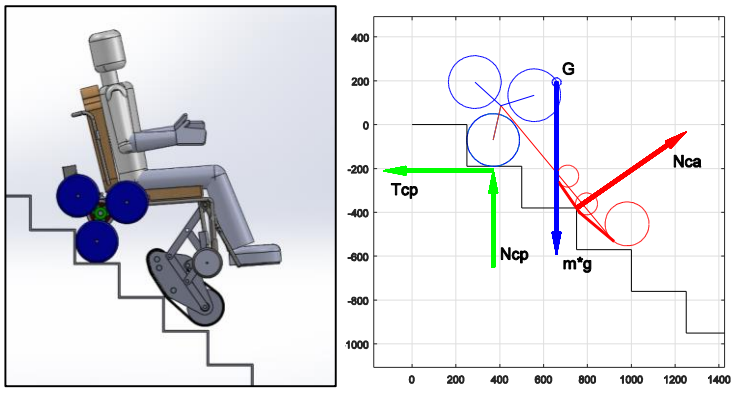

Figure 1 – Free-body diagram of Wheelchair.q on stair

The two contact points are the locomotion unit (on the rear) and the idle track (on the front). The front contact force is oriented as the normal of the track surface on the contact point. In order to avoid slippage, the friction force (Tcp) on the wheel must be almost equal to the horizontal component of the track contact force (Nca). In general, especially for stairs with high slope, the contact force on the track can be high, compromising the static stability. In order to avoid this condition, most of the wheelchair weight must be loaded on the locomotion unit. A possible solution to this problem could be an inverted architecture with the locomotion unit on the front, carrying most of the wheelchair weight, and the idle track on the rear.
The second issue is related to wheelchair oscillation during stair climbing. The use of a rotating leg locomotion is the source of the wheelchair oscillation. During steady state step climbing, the locomotion unit center advances with a not straight trajectory similar to a cycloid, represented in Figure 2.

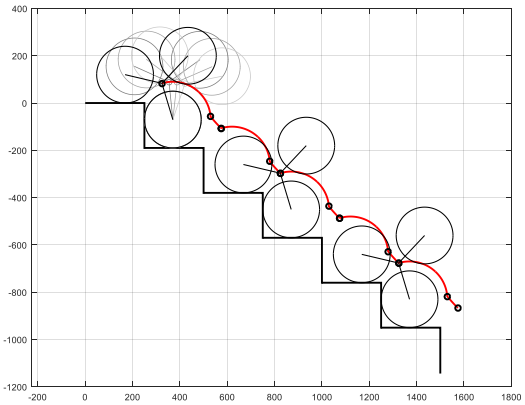

Figure 2 – Trajectory of the locomotion unit center during steady state stair climbing

No active mechanism to control the seat orientation is expected on the wheelchair so the oscillating movement is transmitted to the user reducing the comfort. In early wheelchair concepts, the problem has been faced trying to minimize the oscillation amplitude by choosing appropriately the relative position between locomotion units and track [28]. However, the oscillation cannot be totally canceled and their minimization imposes important constrains to wheelchair design.
A complete compensation of the seat oscillation could be obtained with the introduction of a cam mechanism between the wheelchair frame and the seat that could completely compensate the oscillation related to the locomotion unit motion, at least in a nominal condition. For these reasons, a new wheelchair structure has been designed.

The paper is organized as follow: in *Section 2* the new wheelchair architecture is presented. The functional elements are shortly described and the cam mechanism is introduced. *Section 3* shows the cam mechanism design process. The methodology for obtaining the correct cam profile, starting from the description of the locomotion unit motion is illustrated. In *Section 4* a parametric analysis on the cam mechanism is proposed. The effects of the mechanism parameters on the performances of the cam profile are shown and a procedure to identify the best dimensions for the mechanism is proposed. Finally, in *Section 5* conclusions are stated and future developments of the project are considered.

2. Functional design

In this section the new wheelchair architecture is presented.

2.1 Functional elements

All the wheelchair architectures developed till now are made by three functional elements plus the transmission group. Also the new concept presented in this paper has the same components even if they are arranged in a different way according to the considerations done in the introduction. In Figure 3 a comparison between old and new wheelchair versions is given. The wheelchair functional elements are: locomotion unit (element 1 in Figure 3), seat (2), track (3) and transmission group (4).

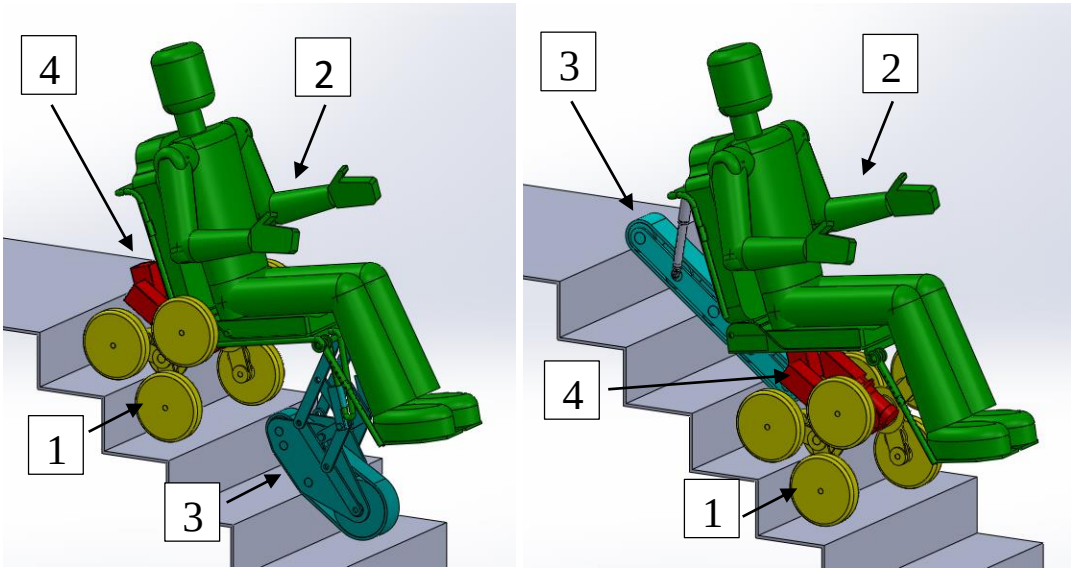

Figure 3 – Wheelchair functional elements in old (left) and new (right) wheelchair versions

The characteristic element of all wheelchair versions and also of all mobile robots presented in [23], [24] and [25] is the triple-wheels locomotion unit. It is composed of a triangular shaped frame with an internal epicyclical transmission as represented in Figure 4.

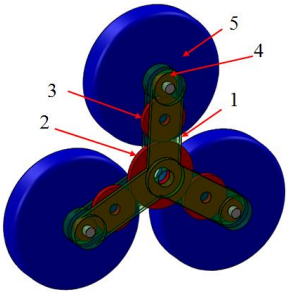

Label	*Component*
1	Planet carrier
2	Solar gear
3	First planet gear
4	Second planet gear
5	Wheel

Figure 4 – Detail of the locomotion unit structure

This structure has two degrees of freedom: the rotation of the solar gears and the revolution of the planet carrier. This feature has been used to develop a smart architecture for mobile robots able to climb obstacles in an autonomous way [23-25]: only one motor is used to control each locomotion unit which behavior is determined by dynamic conditions. In particular, the most relevant result is that the planet carrier revolution starts automatically when the robot hurts an obstacle and the contact friction is able to stop the wheels rotation. For wheelchair applications, the same locomotion unit structure has been used but a different actuation system has been implemented [29]. Due to safety issues, all the degrees of freedom must be controlled and thus two different motors are used to control independently the wheels rotation and the planet carrier revolution. The adopted architecture is represented in Figure 5. Both planet carriers are

connected to the same motor (Mp) in order to have a synchronous rotation while two different motors (Ms) are used to control the solar gear rotation of each locomotion unit.

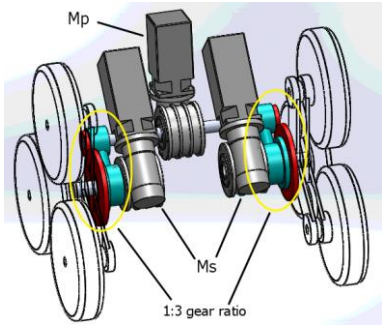

Figure 5 – Detail of the actuation and transmission system

2.2 Wheelchair structure

The wheelchair behavior is affected by the relative positions and connection between the functional elements previously introduced. Indeed, starting from the same functional elements and keeping in mind the considerations done at the end of the introduction, several structures can be designed. The innovation presented in this paper is the introduction of the cam mechanism between the wheelchair frame and the seat in order to filter the oscillation introduced by the locomotion unit motion.

Independently from the specific structure adopted, some preliminary considerations can be done:

- the cam mechanism should be integrated into the wheelchair structure in order to minimize the number of link and coupling;
- the cam follower should be swinging to avoid sliding movement;
- the structure must be as simple as possible with the lower number of moving parts and actuators.

In Figure 6 an architecture for the wheelchair structure is proposed. The cam is fixed with respect to the locomotion units. While the locomotion units rotate performing the step climbing sequence, the cam controls the distance between points R and P according to the designed profile and allows to keep a constant orientation for the seat. The seat moves with a translational motion along a straight line parallel to the line connecting the step edges if the cam mechanism completely compensates the oscillation generated by the locomotion unit motion. In Figure 7 the velocity vectors of remarkable points of the wheelchair structure are presented.

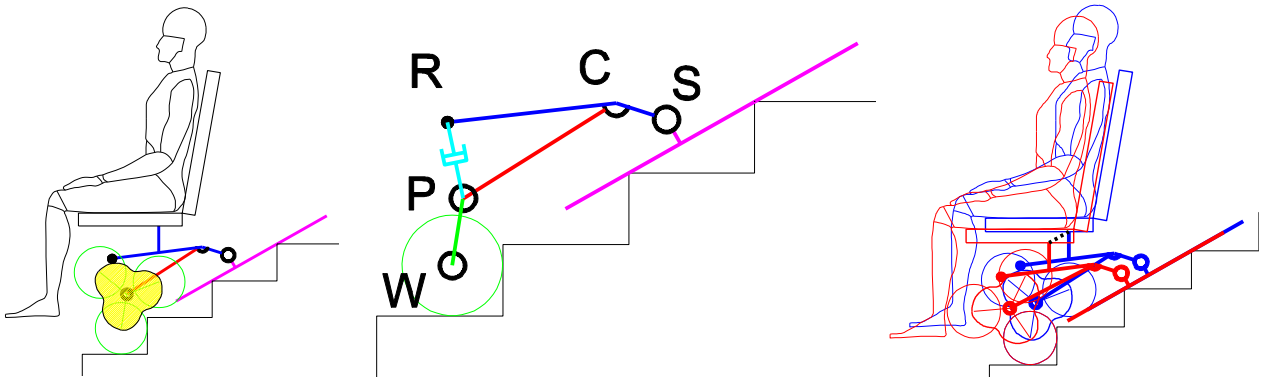

Figure 6 – Wheelchair structure: (a) seat self-levelling cam mechanism; (b) equivalent functional scheme of the cam mechanism; (c) pure translational motion of the seat obtained using the cam mechanism

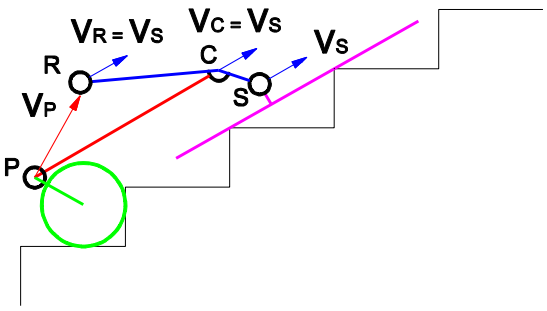

Figure 7 –Velocity vectors for remarkable points of the wheelchair structure

In Figure 8 the wheelchair is represented in the flat ground and stair-climbing configurations. A couple of caster wheels are the rear footholds for the wheelchair during flat ground motions. Moreover, a reconfiguration mechanism is required to set the wheelchair in a configuration proper to stair-climbing. The relative position between the track and the locomotion units should be changed and the caster wheels must be moved in order to avoid contact with step edges. The detailed analysis of these aspects is not the goal of this paper and it will be discussed in future works.

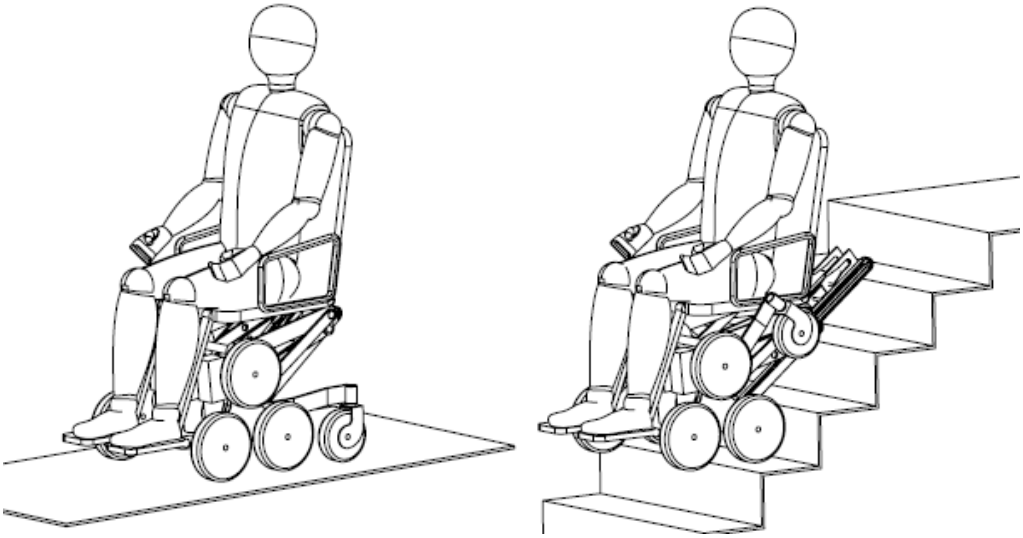

Figure 8 – Wheelchair configurations for movement on flat ground and on stair

2.3 Project requirements

In this sub-section the wheelchair requirements are presented in term of stair typologies that can be climbed. This step is fundamental for identifying the possible set of working conditions and for selecting some reasonable nominal conditions through which generate the cam profile. According to UNI10804 - gen1999, step proportions are unified depending on the application. The Blondel formula is presented in Eq.(1) and it relates the step rise (h_0) with the step tread (P) as represented in Figure 9.

$$2h_0 + P = 620 \div 640 \text{ mm} \quad (1)$$

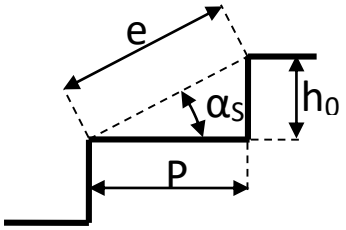

Figure 9 – Schematic representation of a step

Three different step proportions can be derived and are listed in Tab.1.

Table 1 – Standard stair dimensions

	h_0 [mm]	P [mm]	α_S	e [mm]
Low slope	145	350	22.5°	378.8
Medium slope	170	300	29.5°	344.8
High slope	190	250	37°	314

The wheelchair actuation system has been sized to be able to climb all the possible standard stairs belonging to Tab.1. For each stair, the trajectory of the locomotion unit center will be different. This means that it is impossible to design a single cam profile able to completely compensate the seat oscillation in any case. Thus, it is necessary to define a reasonable nominal stair with which design the cam profile. When the wheelchair climbs non-nominal stairs, the oscillation will be only partially compensated by the cam mechanism but the residual could be negligible for a proper choice of the nominal stair.

2.4 Nominal stair

In this sub-section the nominal step dimensions will be defined. Each type of stair can be completely defined by two parameters: stair slope (α_S) and step diagonal (e) as can be observed in Figure 10:

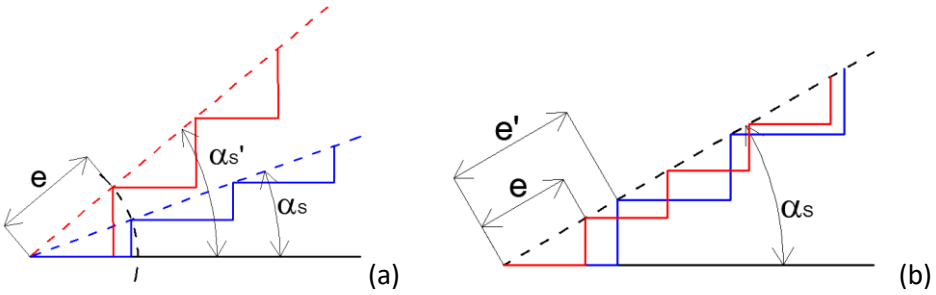

Figure 10 – (a) Stairs with the same step diagonal and different slope; (b) Stairs with the same slope and different step diagonal

In order to remove the dependence from the stair slope in the graphic representation, the stair will be represented rotated by α_S. In this configuration the line connecting the step edges is horizontal.

The trajectory of point P (center of the locomotion unit) is in general complex, as represented in Figure 2, and it depends on the relation between the locomotion unit dimensions and the step proportions. The step geometry that simplifies the process of cam design (i.e. the nominal stair) is the one that generates the simplest trajectory for point P. This condition is obtained when the locomotion unit moves only with consecutive rotations around the blocked wheel of the locomotion unit. It means that after a 120° rotation of planet carrier the front wheel comes in contact with both riser and tread of the following step. In this condition, the trajectory of the locomotion unit center is a sequence of circular arcs as represented in Figure 11 independently from the stair slope. This condition occurs when *e* is equal to the distance between two wheels of the locomotion unit as stated in Eq.(2).

$$e = e_n = l_L\sqrt{3} \cong 277.1 \text{ mm} \qquad \text{with } l_L = 160 \text{ mm} \tag{2}$$

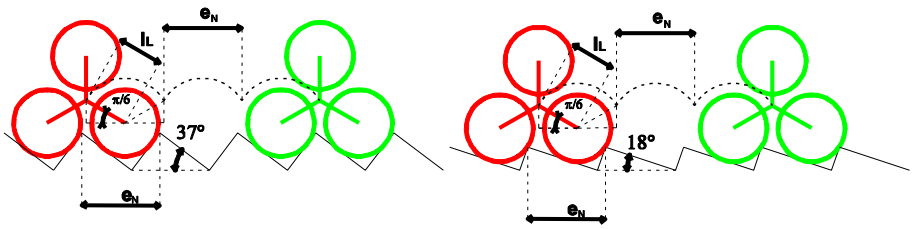

Figure 11 – Representation of the locomotion unit trajectory on nominal stairs with different slopes

The value of the length of the locomotion unit arm (l_L) has been obtained through the scheme of Figure 12 by considering the configuration in which the highest step is climbed with a safety margin in the upper wheel contact. By applying geometrical relations on the scheme of Figure 12, Eq.(3) can be derived. By imposing the maximum climbing step height (h_{0max}) equal to 240 mm [28], the value of l_L can be obtained as showed in Eq.(4). The value imposed for h_{0max} is bigger than the maximum step rise but it can occur with single step climbing such as for sidewalk.

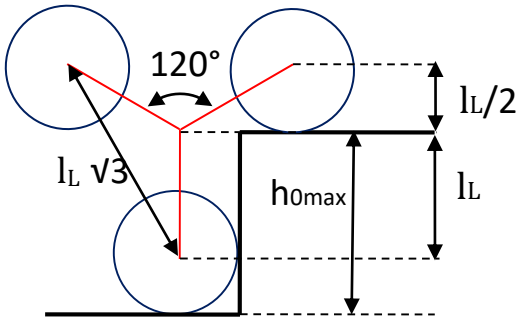

Figure 12 Scheme used to obtain the value of the locomotion unit arm length (l_L)

$$l_L + \frac{l_L}{2} = \frac{3}{2} l_L = h_{0max} \tag{3}$$

$$l_L = \frac{2}{3} 240\ \text{mm} = 160\ \text{mm} \tag{4}$$

Comparing the nominal value of *e* (e_N) from Eq.(2) with the values from Tab.1, it can be observed that the nominal value is lower respect to any values of standard stairs.

From one side this means that the nominal condition cannot be obtained for standard stairs and, therefore, the seat oscillation cannot be fully compensated by the cam mechanism. From the other side, it ensures that the front wheel, after the locomotion unit rotation, leans on the step tread in a stable condition. This is very important for preventing the undesirable behavior that occurs when the upper wheel touches the step riser before the step tread.

Once the nominal e_N value has been calculated, it is necessary to fix the nominal stair slope (α_{SN}) to completely define the nominal stair. For example, the maximum value among standard stairs (α_S = 37°) can be chosen and consequently the values of nominal rise (h_{0N}) and nominal tread (p_N) can be derived from the scheme of Figure 9 and Eq.(5) can be written.

$$\begin{cases} h_{0N} = e_N \sin(\alpha_{SN}) = 166.8\ mm \\ p_N = e_N \cos(\alpha_{SN}) = 221.3\ mm \end{cases} \tag{5}$$

The nominal stair is now completely defined and its dimensions are summarized in Tab.2.

Table 2 - Nominal stair dimensions

	h_0 [mm]	**P [mm]**	**α_S**	**e [mm]**
Nominal stair	*166.8*	*221.3*	*37°*	*277.1*

When the locomotion unit climbs a step with non-nominal dimensions, its motion is no longer a pure rotation around the blocked wheel of the locomotion unit. Referring to Figure 13 a reference configuration (labeled 1 in Figure 13) can be identified. This configuration is the one in which one of the locomotion unit arm is perpendicular to the line connecting the step edges. From this reference configuration, the step climbing sequence can be divided in three phases:

1. From 1 to 2 the locomotion unit has a finite rotation around the pole Q1 up to bring the front wheel in contact with the step riser. The initial and final configurations are completely defined but the exact trajectory cannot be known a priori because it depends on the control logic adopted to manage the two degrees of freedom of the locomotion unit.
2. From 2 to 3 the motion is a finite rotation around the pole Q2 that is the center of the blocked wheel. The rotation amplitude changes with stair dimensions.
3. From 3 to 1 the locomotion unit has a finite rotation around the pole Q3 up to the reference configuration. As in the first phase, the initial and final configurations are known, but the exact trajectory depends on the control strategy.

A possible trajectory for the center of the locomotion unit (point P) during the climbing of a non-nominal stair is represented at the bottom of Figure 13 as a composition of the three phases described above.

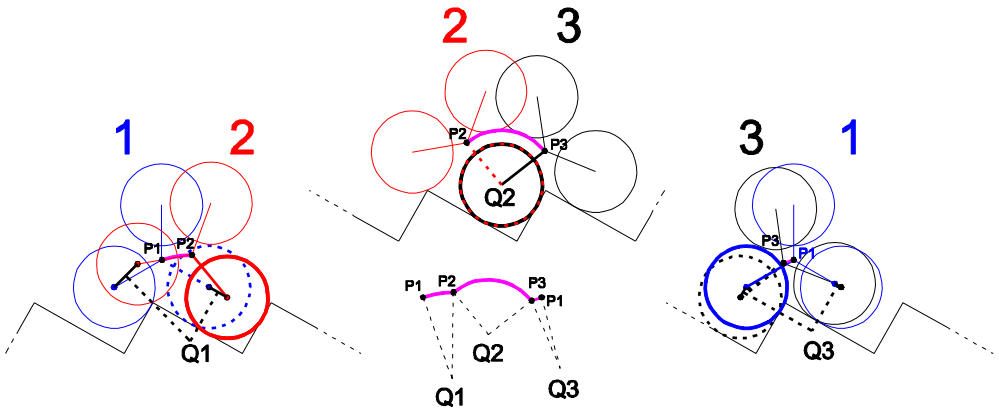

Figure 13 - Representation of the locomotion unit motion on non-nominal stair

3. Cam mechanism design

In the following paragraph the design of the cam mechanism will be presented. As stated in the previous paragraph, the design process will be developed for the nominal stair and the proposed methodology is valid only under this hypothesis. Starting from the mechanical structure presented in Figure 6, the schematic representation of Figure 14 can be derived.

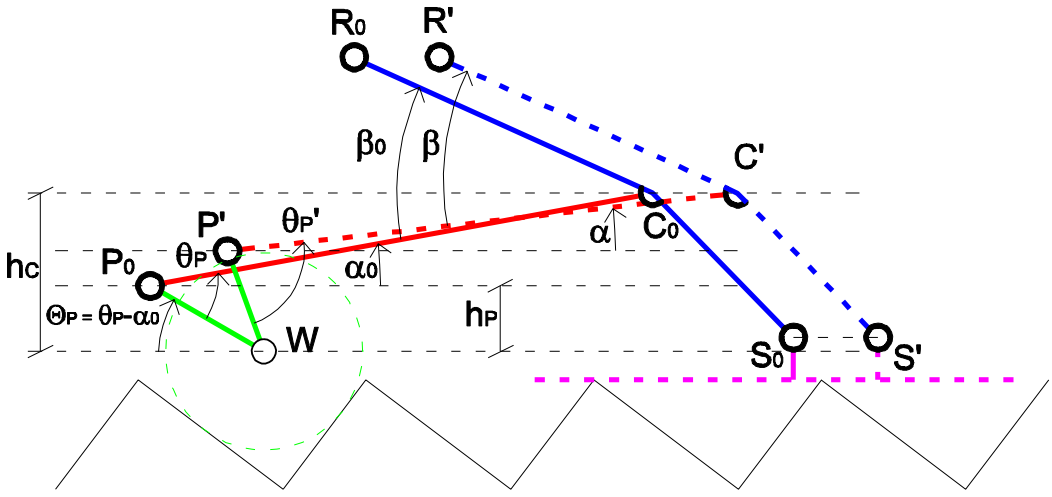

Figure 14 – Schematic representation of the mechanism during stair climbing sequence

The point S, connected with the track that moves along the stair, moves on a straight trajectory parallel to the line connecting the step edges. The cam profile must be designed such that the distance between point P and R changes properly in order to maintain a constant orientation for the seat (i.e. a constant orientation for the element RC). According to this hypothesis the point C moves on a straight trajectory parallel to point S trajectory. At the same time, the locomotion unit rotates around the fixed wheel (point W) and its center (point P) moves on a circular trajectory that can be described by Eq.(6) that has been derived from the scheme of Figure 14.

$$h_P = l_L \sin(\Theta_P) = l_L \sin(\theta_P - \alpha) \tag{6}$$

For a generic locomotion unit rotation θ_P, the wheelchair frame (PC) rotates of $\Delta\alpha = \alpha - \alpha_0$. Angle β is the angle that must be controlled by the cam mechanism in order to compensate the seat oscillation. Starting from the initial value β_0 that will be chosen properly, for each position of the locomotion unit, $\Delta\beta = \beta - \beta_0$ must be equal and opposite to Δα to maintain a constant orientation of the seat.

From the scheme of Figure 15, the relation between α and θ_P can be obtained: Eq.(7) and Eq.(8) can be derived by applying the cosine and the sine theorem on triangle WPC. Finally, by considering triangle WHC, the value of α can be obtained as in Eq.(9).

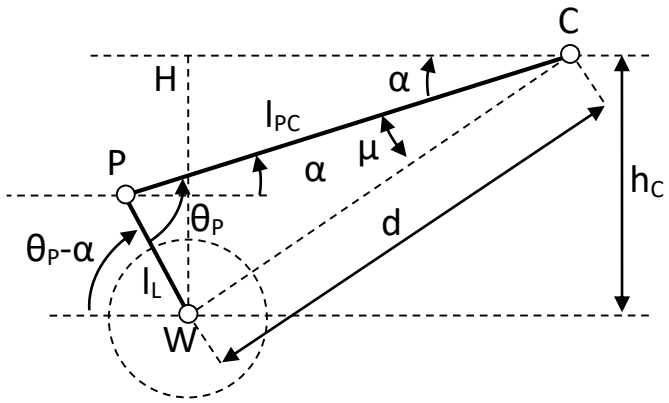

Figure 15 – Schematic representation of the mechanism during locomotion unit rotation on stair (detail)

$$d(\theta_P) = \sqrt{l_{PC}^2 + l_L^2 - 2 l_{PC} l_L \cos\theta_P} \tag{7}$$

$$\mu(\theta_P) = \sin^{-1}\left(\frac{l_L}{d}\sin\theta_P\right) \tag{8}$$

$$\alpha = \sin^{-1}\left(\frac{h_C}{d}\right) - \mu \tag{9}$$

A first consideration deals with the proper choice of the relative position between points P and C. The wheelchair oscillation (represented by Δα) can be minimized with a proper choice of the position of point C. The synthesis of the cam profile will be easier with small values of Δα because the resulting angular displacement for the cam (Δβ) will be smaller. The two parameters that affect the wheelchair oscillation are l_{PC} and h_C. It can be observed that the smaller values of Δα can be obtained with:

- l_{PC} as higher as possible compatibly with the wheelchair dimension;
- h_C as the mean value with respect to the minimum and maximum values of h_P.

$$h_{P\,min} = \frac{l_L}{2} \quad h_{P\,max} = l_L \quad h_{C\,opt} = \frac{3}{4} l_L$$

The first statement can be justified observing that a higher value of l_{PC} brings to a lower rotation Δα, starting from the same variation of h_P. The second statement can be understood observing Figure 16. During step climbing the point C move along a straight line. By choosing a generic initial position C_0 (i.e. choosing a value

for h_C) the oscillation Δα can be evaluated in Figure 16 by drawing the line CP'' that represents the initial configuration (C_0P_0) with respect to CP'. The minimum value of oscillation Δα is obtained when the distance P'P'' is minimum. This condition is represented by the * configuration and occurs when $h_C^* = h_{C\,opt}$.

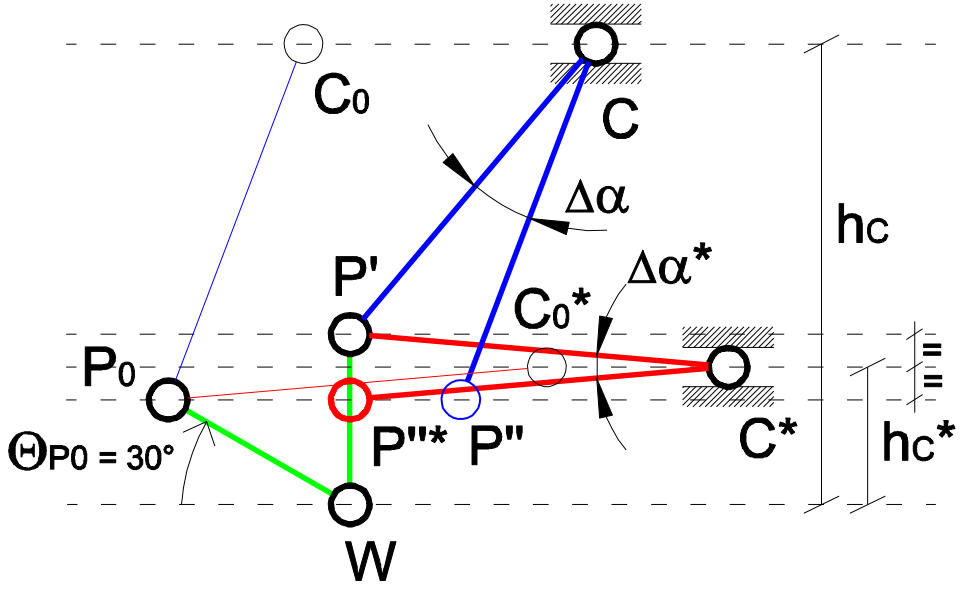

Figure 16 – Graphic analysis for the choice of the best position for point C

Each step climbing can be modeled as a 120° rotation of the locomotion unit. In Figure 17 the initial, final and intermediate configurations are represented with the parameter h_C chosen at its most favorable value.

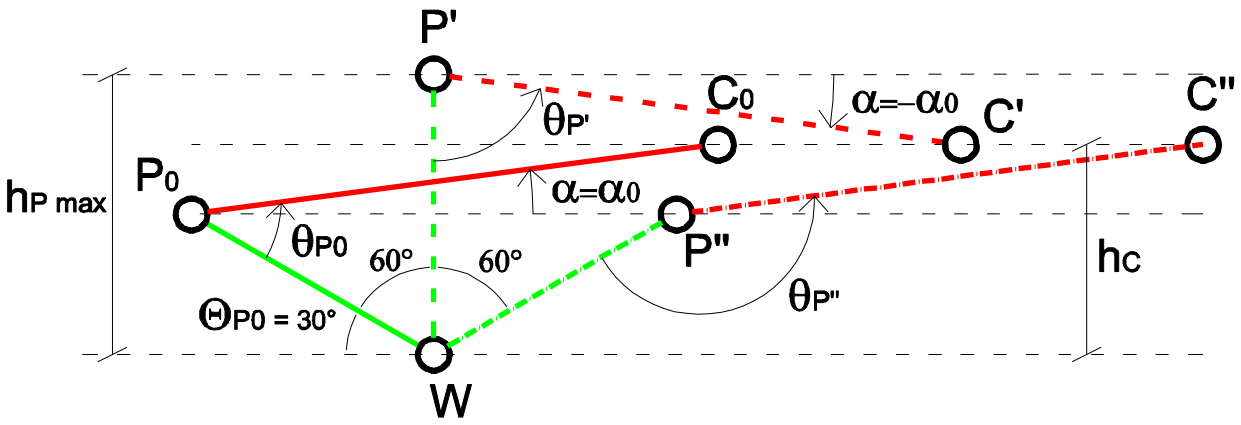

Figure 17 – Representation of the mechanism during an entire step climbing sequence

With this hypothesis, the total wheelchair oscillation is $\Delta\alpha = 2\alpha_0$ and a qualitative trend for $\alpha(\theta_P)$ is represented in Figure 18. An important observation can be done on the asymmetric shape of the function. The maximum value for h_P (minimum value for α) is obtained after a rotation of 60° of the locomotion unit. In this configuration $\theta_P = \theta'_P$ and its value can be obtained through the set of expressions of Eq.(10) that has been derived from Figure 17.

$$\begin{cases} \theta'_P = \Theta'_P + \alpha' = \Theta'_P - \alpha_0 \\ \theta'_P = \Theta_{P0} + 60° - \alpha_0 \\ \Theta_{P0} = \theta_{P0} - \alpha_0 \\ \theta'_P = \theta_{P0} + 60° - 2\alpha_0 \end{cases} \tag{10}$$

This means that for a rotation of 60° of the locomotion unit, the angle θ_P increases of a lower amount than 60°. Moreover, at the end of the locomotion unit rotation $\theta_P = \theta_P''$ as expressed by Eq.(11) and its value can be derived from Eq.(10) and the scheme of Figure 17 as expressed in Eq.(11).

$$\begin{cases} \theta_P'' - \theta_{P0} = 120° \\ \theta_P'' = \theta_{P0} + 120° \\ \theta_P'' = \theta_P' - 60° + 2\alpha_0 + 120° \\ \theta_P'' = \theta_P' + 60° + 2\alpha_0 \end{cases} \tag{11}$$

In Figure 18 the trend of $\beta(\theta_P)$ is also represented. In order to completely compensate the oscillation introduced on the wheelchair frame, for each value of θ_P the variation of the seat orientation should be equal and opposite to the variation of the wheelchair frame orientation. Thus, the function that describes the trend of $\beta(\theta_P)$ can be obtained from the function $\alpha(\theta_P)$ as in Eq.(12).

$$\begin{cases} \Delta\beta = \beta(\theta_P) - \beta_0 \\ \Delta\alpha = \alpha(\theta_P) - \alpha_0 \\ \Delta\beta = -\Delta\alpha \end{cases} \quad \rightarrow \quad \beta(\theta_P) = \beta_0 + \Delta\beta = \beta_0 - \Delta\alpha = \beta_0 - \alpha(\theta_P) + \alpha_0 \tag{12}$$

The initial value β_0 is a parameter that should be chosen properly because it affects the shape and the dimension of the cam profile. A first observation can be done on the minimum acceptable value for β. In order to have a positive radius of the cam, β must be greater than zero for any values of θ_P. This affects the choice of β_0 that must be greater than Δα.

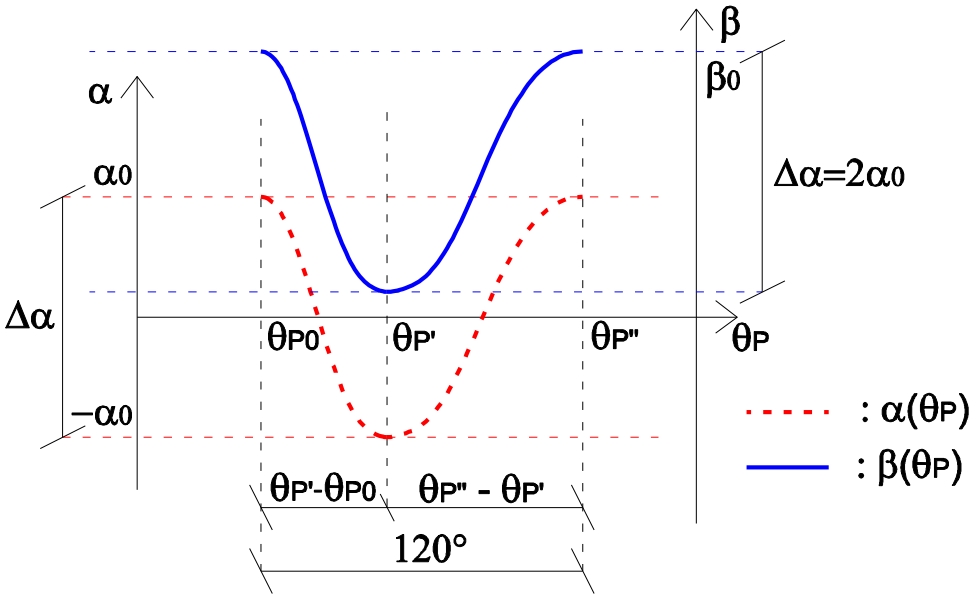

Figure 18 – Trend of α(θ_P) and β(θ_P)

Once these preliminary concepts have been fixed, the procedure for the cam design can be described.
In Figure 19 two different configurations for the mechanism are showed in the kinematic inversion in which the locomotion unit and the cam connect with it are fixed. Variables with subscript zero refer to the initial configuration of the climbing sequence. The notation with apostrophe indicates variable values in a different and generic configuration of the mechanism. According to this kinematic inversion, during the locomotion unit rotation the wheelchair frame PC moves around P with a rotation of $\Delta\theta_P = \theta_P' - \theta_{P0}$. Meanwhile the seat RC rotates around P and moreover the relative orientation between PC and RC changes according to the

desired angle $\beta(\theta_P)$, in order to remove the oscillation of the seat. The trajectory of point R around P describes the desired cam profile.

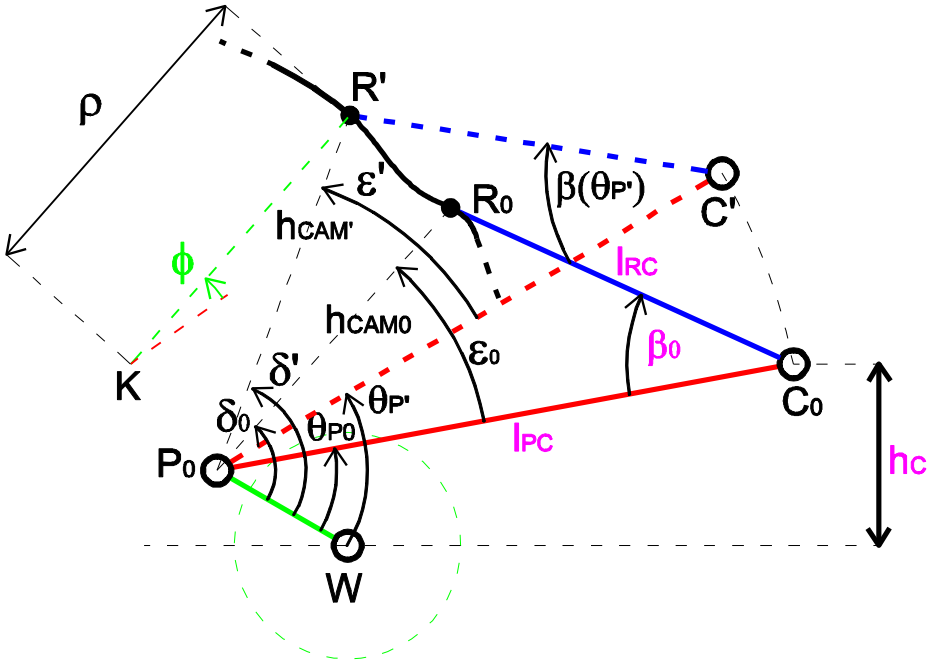

Figure 19 – Scheme used to obtain the cam profile starting from $\beta(\theta_P)$ function

The cam profile can be described in polar coordinates (h_{CAM}, δ) with respect to a reference frame fixed on the locomotion unit and centered in P. By applying the cosine and the sine theorems on triangle $P_0C'R'$ of Figure 19, Eq(13) and Eq.(14) can be derived. Finally, Eq.(15) can be written through geometric considerations on the scheme of Figure 19. These equations define the polar coordinates of the profile, starting from the mechanism and the wheelchair parameters (l_{PC}, l_{RC}, β_0, h_C).

$$h_{CAM} = \sqrt{l_{PC}^2 + l_{RC}^2 - 2 l_{PC} l_{RC} \cos\beta} \tag{13}$$

$$\varepsilon = \sin^{-1}\left(\frac{l_{RC}}{h_{CAM}} \sin\beta\right) \tag{14}$$

$$\delta = \varepsilon + \theta_p \tag{15}$$

In summary, the cam design process can be related to the synthesis of a motion generator cam mechanism as defined in [30] that imposes a straight line translational motion to the output link RC.

4. Parametric analysis on the cam mechanism

The procedure described in the previous paragraph defines a cam profile capable of removing the seat oscillation at least for the nominal stairs. Different profiles can be obtained changing the mechanism parameters. By following the proposed procedure, it is possible to obtain a constant orientation for the seat during stair-climbing for any combination of parameters. However, the resulting cam profile will be different and thus different performances should be expected. In this section a parametric analysis on the cam mechanism will be conducted with the aim of analyzing the relations of the different parameters with the cam dimensions and the mechanism performances. The results can be used to properly choose the best cam mechanism. In Figure 20 the mechanism is represented in another kinematic inversion in two different

configurations: the initial one ($P_0C_0R_0$) and the configuration associated with the maximum value for h_P (P_0C_0R'), that corresponds to the maximum value of $\Delta\alpha$ and to the minimum values of β and h_{CAM}. The wheelchair frame PC is fixed, the seat RC rotates around C and the cam and the locomotion unit rotate around P. This representation can be associated with the generic representation of a cam mechanisms with swinging follower.

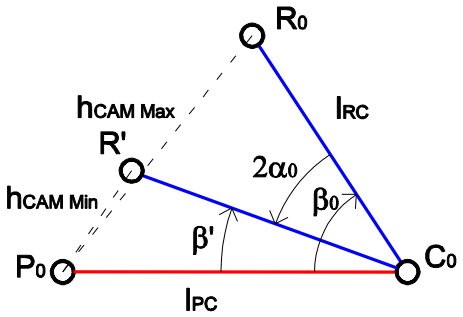

Figure 20 – Generic representation of a cam mechanisms with swinging follower in two reference configurations

The mechanism (see Figure 19) has four independent parameters: l_{PC}, l_{RC}, β_0 and h_C.
The other quantities are functions of these parameters, as can be observed in Eq.(13), Eq.(14) and Eq.(15). The parameter h_C has been fixed to the best value according to Figure 16. The remaining three parameters can be redefined by introducing the dimensionless quantities as in Eq.(16).

$$R = \frac{l_{RC}}{l_{PC}} \qquad I = \frac{l_{PC}}{l_L} \tag{16}$$

The parameters R and β_0 change the cam shape while I affects the mechanism dimension respect to the locomotion unit size.
A complete analysis of the cam mechanism cannot be done only focusing on the dimension and geometry of the cam profile. Important quantities that must be taken into account are the pressure angle (θ_{PRESS}) and the radius of curvature (ρ). According to [31], Eq.(17)-(20) can be written. These equations are known from the cam mechanism synthesis theory and can be understood referring to Figure 19. In details, Eq.(17) allows the computation of the pressure angle of the cam profile from the geometry of the mechanism. The angle β represents the angle between the frame PC and the rocker arm RC, while K is the center of curvature of the pitch curve. Then, further parameters can be introduced: the radius of curvature (ρ), and the angle ϕ that represents the angle between the segment KC and the direction defined by the frame PC. The Eq.(19) allows calculating the radius of curvature while Eq.(18) and Eq. (20) define the angle ϕ and its first derivative. The value of the pressure angle (θ_{PRESS}) and the value of the radius of curvature of the cam profile (ρ) describe the performances of the cam and will be used to evaluate the quality of the profiles designed through the parametric analysis.

$$\theta_{PRES} = \frac{\pi}{2} - \beta - \phi \tag{17}$$

$$\tan\phi = \frac{l_{RC}\sin\beta\,(1-y')}{l_{PC} - l_{RC}\cos\beta\,(1-y')} = \frac{\sin\beta\,(1-y')}{1/R - \cos\beta\,(1-y')} \tag{18}$$

$$\rho = \frac{l_{PC} - l_{RC}\cos\beta\,(1-y')}{(1+\phi')\cos\phi} \tag{19}$$

$$\phi' = \frac{l_{RC}(1-y')y'\cos(\beta+\phi) - l_{RC}y''\sin(\beta+\phi)}{l_{PC}\cos\phi - l_{RC}(1-y')\cos(\beta+\phi)} \tag{20}$$

The function representing the angular displacement is defined by $y = \beta(\theta_P)$ and its first and second derivatives are stated in Eq.(21) and Eq.(22).

$$y' = \frac{dy}{d\theta_P} = \frac{d\beta}{d\theta_P} = \frac{d(\beta_0 + \alpha - \alpha_0)}{d\theta_P} = \frac{d\alpha}{d\theta_P} \tag{21}$$

$$y'' = \frac{d^2y}{d{\theta_P}^2} = \frac{d^2\alpha}{d{\theta_P}^2} \tag{22}$$

For cam mechanisms with swinging follower the most critical issues are related to the pressure angle rather than the radius of curvature. In order to avoid the mechanism block due to a critical force transmission, the higher value of the pressure angle during the rising phase must be lower than 45°÷50° [31]. In this particular application, the cam mechanism can rotate in both directions depending on whether the wheelchair is going up or down stair. Referring to Figure 18 each of the two parts of the rocker arm motion can be either a rising or a falling phase. In conclusion, the design condition as regard the pressure angle can be express by the relation of Eq.(23).

$$\max(\,|\,\theta_{PRESS}\,|\,) \leq \theta_{PRESS\,LIMIT} \qquad \theta_{PRESS\,LIMIT} = 45° \div 50° \tag{23}$$

In general, the pressure angle decreases with the rise of the cam size. In order to reduce the number of free parameters, the size of the cam can be fixed. A bigger cam is preferable for reducing the problems related to pressure angle. Thus, it could be useful to impose the maximum acceptable dimension for the cam considering the interference between the cam and the step edges. Referring to Figure 20 it can be observed that the maximum cam radius ($h_{CAM\,Max}$) corresponds to the initial condition where the value of β is maximum and equal to β_0. In this configuration the relation expressed in Eq.(24) can be written by applying the cosine theorem on triangle $P_0R_0C_0$ of the scheme of Figure 20.

$$h_{CAM\,Max}^2 = l_{PC}^2 + l_{RC}^2 - 2l_{PC}l_{RC}\cos\beta_0 \tag{24}$$

Introducing in Eq.(24) the dimensionless parameters from Eq.(16), one has:

$$\frac{D^2}{I^2} = R^2 - 2R\cos\beta_0 + 1 \qquad where \quad D = \frac{h_{CAM\,Max}}{l_L} \tag{25}$$

This means that once the value of parameters D, R and I are chosen, a cam with the desired dimension can be designed by choosing the proper value of β_0 according to Eq.(26) that has been obtained by inverting Eq.(25).

$$\beta_0 = \cos^{-1}\left(\frac{R^2 + 1 - {D^2}/{I^2}}{2R}\right) \tag{26}$$

The desired cam dimension cannot be obtained with any choice of parameters D, R and I. Indeed, Eq.(26) imposes a constrain on the acceptable values for R because the argument of the arccosine function must be included between -1 and 1. Moreover, according to Figure 18, in order to have a positive cam radius, the minimum acceptable value for β_0 must be greater than $2\alpha_0$. These two conditions applied on Eq.(26), bring to the set of relations written in Eq.(27) that constrains the admissible values for R.

$$\begin{cases} 2\alpha_0 < \cos^{-1}\left(\dfrac{R^2 + 1 - {D^2}/{I^2}}{2R}\right) \\ -1 \leq \dfrac{R^2 + 1 - {D^2}/{I^2}}{2R} \leq 1 \end{cases} \tag{27}$$

In summary, the choice of a proper cam profile can be conducted following the flow chart presented in Figure 21.

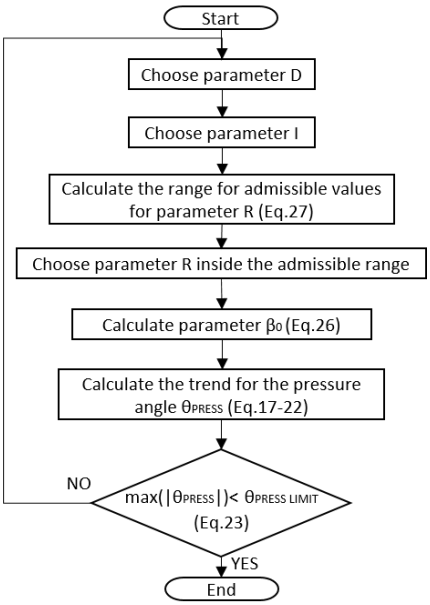

Figure 21 – Flow chart for the choose of a proper cam profile

A proper cam profile satisfies the requirement for the pressure angle and it is suitable as regard the maximum dimension. In order to perform a reasonable choice for the free parameters (D, I and R) a parametric analysis must be conducted.

The first choice regards the parameter D. It has been observed that greater values allow reducing the pressure angle. A first attempt can be done choosing D=1. This means that the maximum radius of the cam is equal to the locomotion unit arm length. After this preliminary choice, the other parameters can be evaluated according to the proposed flow chart.

The dimensionless pitch curve and the pressure angle (θ_{PRESS}) as a function of θ_P for different choices of I, R and β_0 are showed in Figure 22 and Figure 23. These figures allow to have a general overview of the influence of the mechanism parameters over two fundamental aspects in the cam design: profile shape and pressure angles.

Figure 22 illustrates some examples for the dimensionless pitch curves for different combinations of parameters. Note that all the curves have some similarities: the maximum dimensionless radius is the same and each pitch curve is composed of three identical profiles. This happens because the input for the cam synthesis is the single step climbing that requires a 120° of locomotion unit rotation. This means that the corresponding pitch curve will be developed in 120° and the complete shape is the juxtaposition of three identical profiles that correspond to a 360° of locomotion unit rotation and three steps climbing.

Moreover, it appears that the geometrical parameters of the mechanism strongly affect the designed cam shapes and its orientations. Thus, it is fundamental to verify that the chosen parameters are such that no interferences with step edges occurs during stair-climbing.

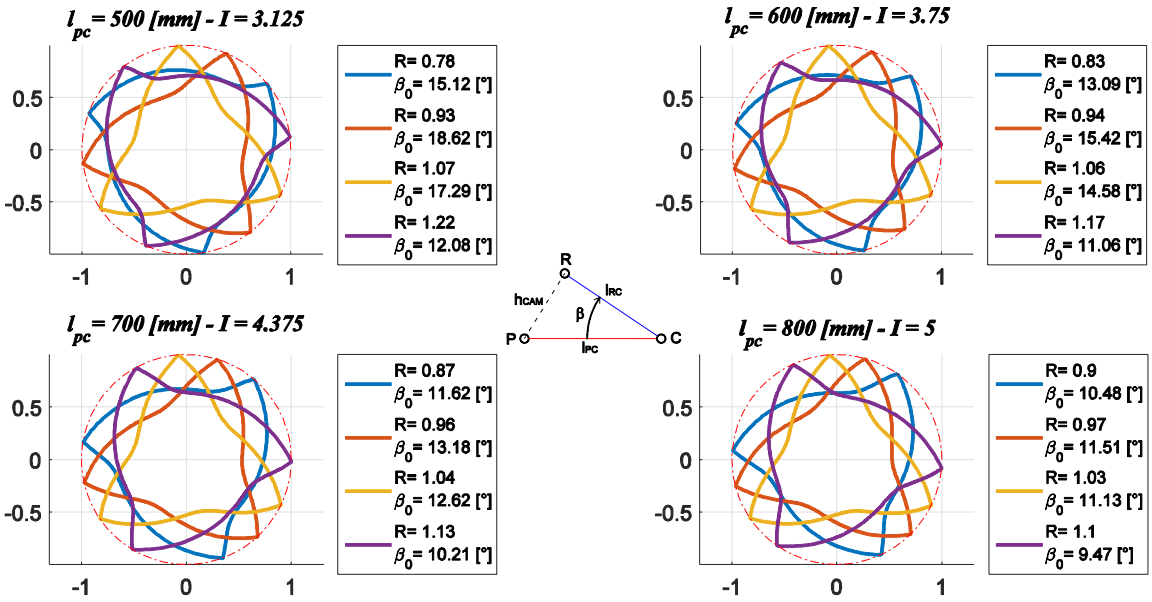

Figure 22 – Dimensionless pitch curve for different combinations of parameters $I = \frac{l_{PC}}{l_L}$, $R = \frac{l_{RC}}{l_{PC}}$, β_0 *with* $D = \frac{h_{CAM\,Max}}{l_L} = 1$

Figure 23 shows the trend of $\theta_{PRESS}(\theta_P)$ during a step climbing sequence. The changing in the mechanism parameters (I, R and β_0) causes significant modifications in the curves. Even if the shape of the curves is almost similar, their positions about the horizontal axis change considerably, affecting the maximum and minimum values for the pressure angle.

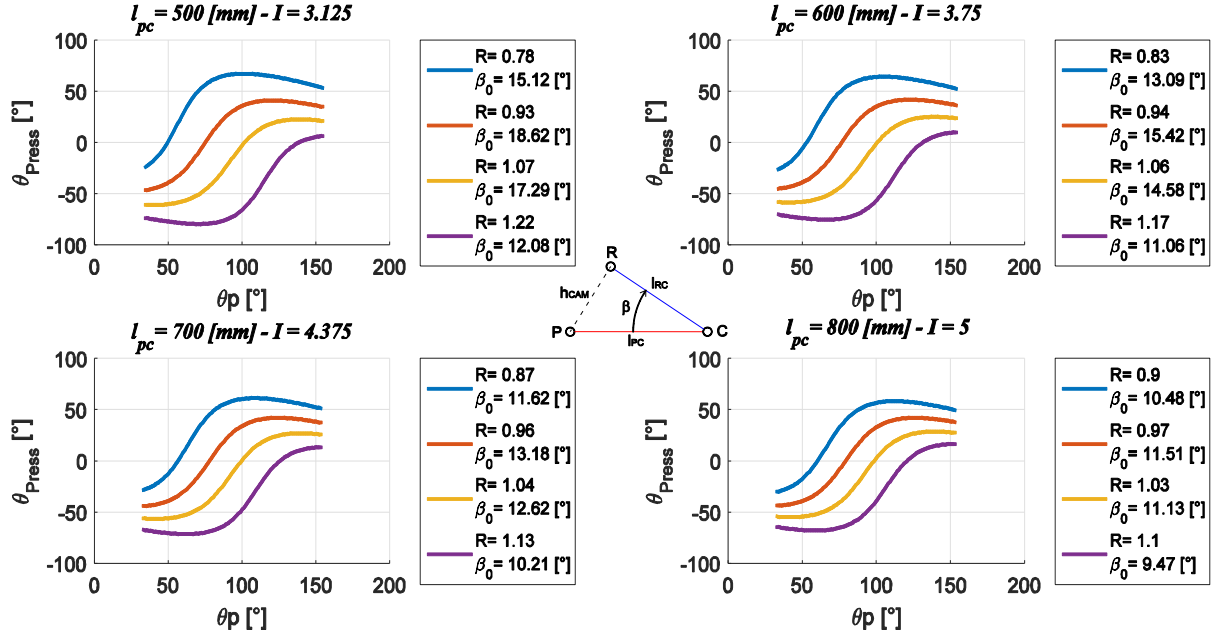

Figure 23 – Trend of $\theta_{PRESS}(\theta_P)$ *for different combinations of parameters* $I = \frac{l_{PC}}{l_L}$, $R = \frac{l_{RC}}{l_{PC}}$, β_0 *with* $D = \frac{h_{CAM\,Max}}{l_L} = 1$

After these first general considerations, a deeper analysis was conducted to select the set of parameters that minimize the maximum value for the pressure angle. In Figure 24 a synthesis of the results is given with a greater number of sample for parameters I (that means for l_{PC}) and R. The analysis of the results was simplified by considering only the max(|θ_{PRESS}|) value instead of the entire $\theta_{PRESS}(\theta_P)$ function. In fact, only the maximum of the pressure angle absolute value is interesting from the parametric analysis point of view. The

whole $\theta_{PRESS}(\theta_P)$ function was analyzed only to get some general information about the influence of the mechanism parameters on the pressure angle.

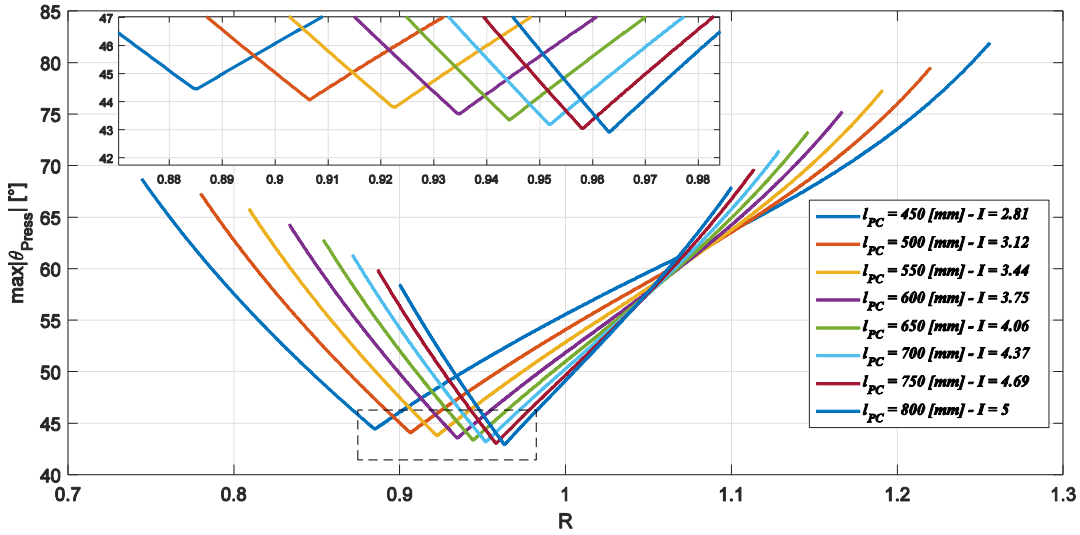

Figure 24 – Trend of max($|\theta_{PRESS}|$) *for different combinations of parameters* $I = \frac{l_{PC}}{l_L}$ *and* $R = \frac{l_{RC}}{l_{PC}}$ *with* $D = \frac{h_{CAM\,Max}}{l_L} = 1$

The trend of max($|\theta_{PRESS}|$) with respect to R have a minimum for any value of I. The value of R that corresponds to the minimum changes with I. Also the minimum value of max($|\theta_{PRESS}|$) slightly changes with I but is always between 43° and 45° as can be observed in the detail of Figure 24. In particular, this value is lower for the higher values of I. Finally, Figure 25 represents the trend of the optimal β_0 as obtained in Eq.(26), with different combinations of R and I and with D=1. The circles identify the values of β_0 for the minima of Figure 24.

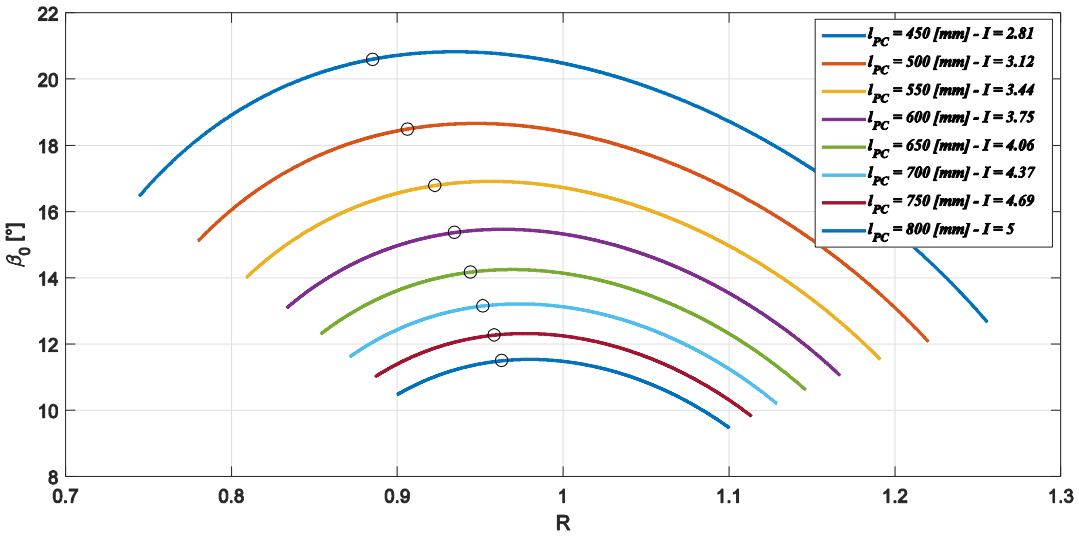

Figure 25 - Trend of optimal β_0 *for different combinations of parameters* $I = \frac{l_{PC}}{l_L}$ *and* $R = \frac{l_{RC}}{l_{PC}}$ *with* $D = \frac{h_{CAM\,Max}}{l_L} = 1$
(the circles identify the values of β_0 for the minima of Figure 24)

For each value of I, that means for each value of l_{PC}, the results obtained show that a minimum value for max($|\theta_{PRESS}|$) can be obtained with a specific pair of values R and β_0 linked by Eq.(26).
In Figure 26, for each value of I, the pitch curve obtained with the pair of R and β_0 that minimize max($|\theta_{PRESS}|$) is represented. It is possible to observe that all the profiles have the same size and are similar in terms of shape and orientation with respect to the locomotion unit frame. Thus, the choice of the best value for I should be done through different considerations.

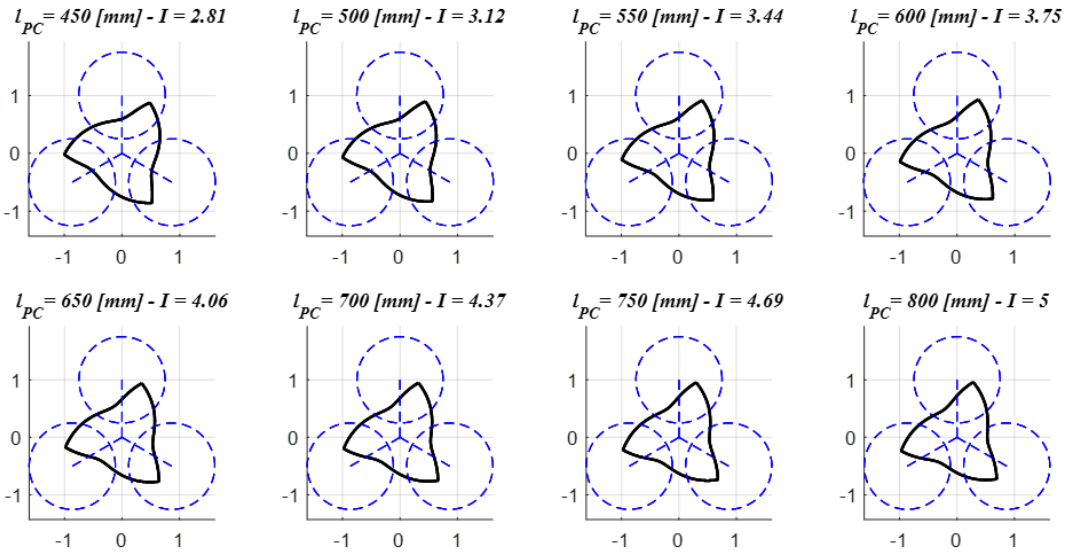

Figure 26 – Optimum pitch curves for different values of $I = \frac{l_{PC}}{l_L}$

Higher values of I are advisable for two reasons. First of all, for the nominal stairs, higher values reduce the initial wheelchair oscillation (Δα) as can be observed in Figure 27. Thank to this effect the angular displacement for the cam mechanism is reduced. Moreover, even for non-nominal stairs, higher values of I reduce the amplitude of the uncompensated oscillation. Finally, the pressure angle is lower even if this effect is less evident (see Figure 24).

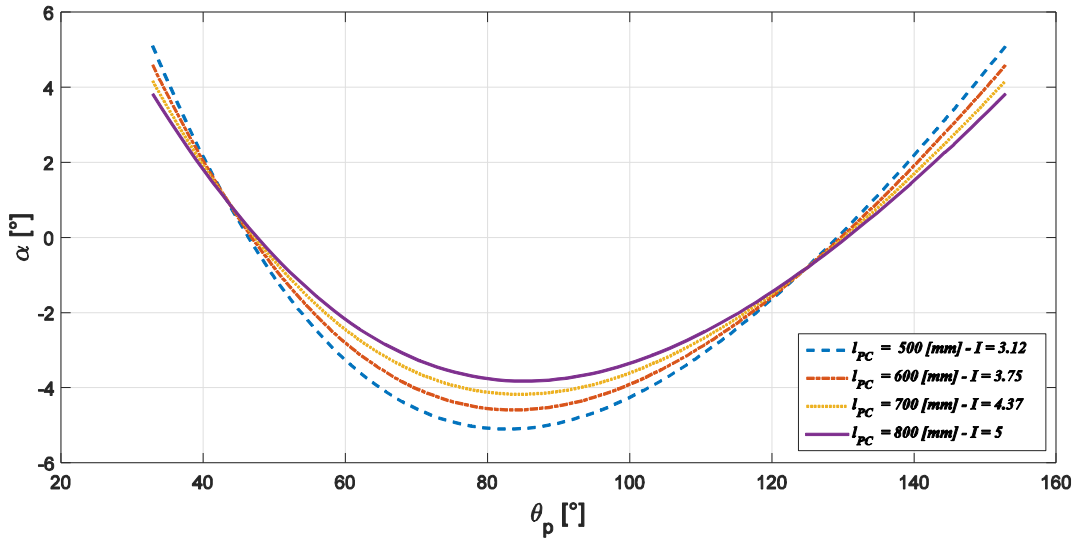

Figure 27 – Trend of α(θP) *for different values of* $I = \frac{l_{PC}}{l_L}$

In conclusion, an optimal choice can be done selecting the highest admissible value for I, that means the highest admissible value for l_{PC}, and choosing the other parameters with the algorithm described in this section. With respect to the range of values taken into account for the parametric analysis, the choice of $l_{PC} = 800$ mm (I = 5) represents the best solution with respect to the overall wheelchair dimension. Consequently, R = 0.96 and β_0 = 11.5° complete the definition of the mechanism. In Tab.3, a summary of the chosen parameters is presented.

Table 3 – Optimal set of mechanism parameters

Parameter	l_{PC}	R	l_{RC}	β_0	max(|θ_{PRESS}|)	I	D

Value	800 mm	0.96	768 mm	11.5°	43.0°	5	1

The pitch curve, designed through the proposed algorithm, has been obtained considering a roller with zero radius. The real mechanism must have a roller with finite radius, thus the cam profile must be calculated. The pitch curve has also a problem related to cusps because it has a discontinuous derivative and generate a self-intersecting cam profile. This is due to the shape of function $\alpha(\theta_P)$ that has finite derivatives at initial and final points. In order to solve this problem, it is necessary to create a smoothed function $\alpha^*(\theta_P)$ that must be considered as the initial input to generate the cam profile. Referring to Figure 28.a, the $\alpha^*(\theta_P)$ curve has been obtained by substituting a smoothing function to curve $\alpha(\theta_P)$ in the initial and final parts for an interval that is the 20 % of the total $\Delta\theta_P$ as explained in Eq.(28).

$$\theta_{P1} - \theta_{Pi} = \theta_{Pf} - \theta_{P2} = 0.2 \cdot (\theta_{Pf} - \theta_{Pi}) \tag{28}$$

The curve smoothing can be improved by increasing this interval, but the error done in the approximation will rise as drawback. Considering the function $\alpha^*(\theta_P)$ instead of $\alpha(\theta_P)$ generates oscillation on the wheelchair seat even on nominal stairs, because the cam profile is no longer able to completely compensate the locomotion unit movement in its initial and final section. In Figure 28.b the amplitude of the seat oscillation due to the proposed cam profile smoothing is showed and it can be observed that it is lower than 1°. The benefits that the use of a smoothed function introduces in the dynamics of the mechanism prevail on the small error generated on the compensation of the frame oscillation.

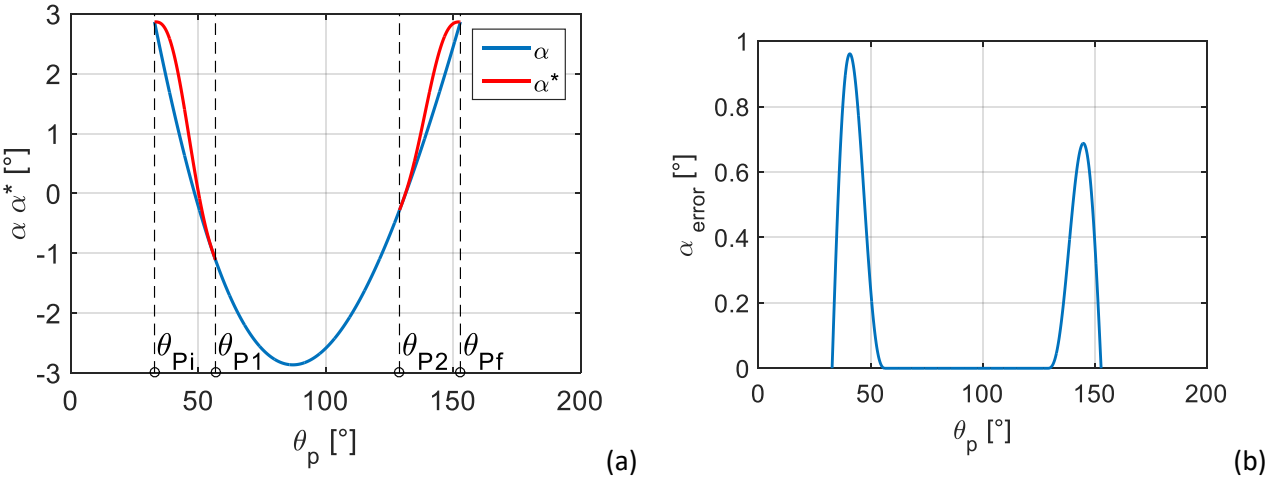

Figure 28 – (a) Comparison between real and smoothed function $\alpha(\theta_P)$; (b) *Amplitude of seat oscillation due to cam profile smoothing*

The $\alpha^*(\theta_P)$ function is composed of two fifth order polynomial curves with different coefficients. The fifth order is necessary to allow choosing six coefficients and imposing the curve continuity, the first and second derivatives continuity both in the external and internal boundary for each interval. The approach is identical for both intervals and it will be showed just for the first section. By imposing the boundary conditions on a generic fifth order polynomial for the angle (α), the velocity (α') and the acceleration (α'') on internal and external boundaries, the linear system of Eq.(29) can be written and the polynomial coefficients C_1, C_2, C_3, C_4, C_5 and C_6 can be obtained by solving it.

$$\begin{cases} C_1\theta_{Pi}^5 + C_2\theta_{Pi}^4 + C_3\theta_{Pi}^3 + C_4\theta_{Pi}^2 + C_5\theta_{Pi} + C_6 = \alpha(\theta_{Pi}) \\ C_1\theta_{P1}^5 + C_2\theta_{P1}^4 + C_3\theta_{P1}^3 + C_4\theta_{P1}^2 + C_5\theta_{P1} + C_6 = \alpha(\theta_{P1}) \\ 5C_1\theta_{Pi}^4 + 4C_2\theta_{Pi}^3 + 3C_3\theta_{Pi}^2 + 2C_4\theta_{Pi} + C_5 = 0 \\ 5C_1\theta_{P1}^4 + 4C_2\theta_{P1}^3 + 3C_3\theta_{P1}^2 + 2C_4\theta_{P1} + C_5 = \alpha'(\theta_{P1}) \\ 20C_1\theta_{Pi}^3 + 12C_2\theta_{Pi}^2 + 6C_3\theta_{Pi} + 2C_4 = 0 \\ 20C_1\theta_{P1}^3 + 12C_2\theta_{P1}^2 + 6C_3\theta_{P1} + 2C_4 = \alpha''(\theta_{P1}) \end{cases} \quad (29)$$

In Figure 29 a comparison between the pitch curve obtained using $\alpha(\theta_P)$ function and the smoothed pitch curve obtained using $\alpha^*(\theta_P)$ can be observed.

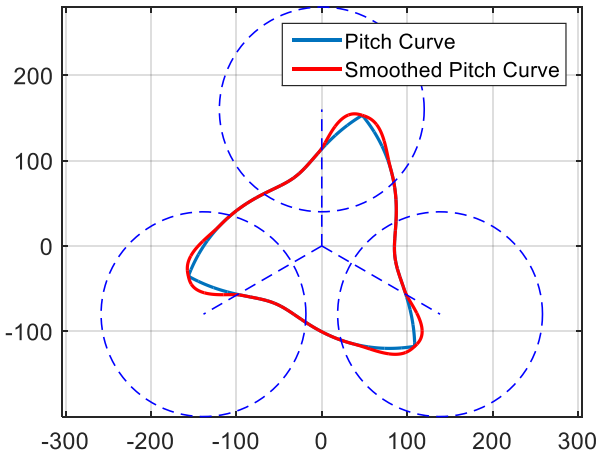

Figure 29 – Comparison between the pitch curve and the smoothed pitch curve

Finally, by introducing a roller with finite radius, the polar coordinates of the cam profile can be obtained through Eq.(30) and Eq.(31) that are taken from the classical cam mechanism theory [31]. The polar coordinates of the pitch curve (h_{CAM}, δ) have been given in Eq.(13) - (15). The real profile coordinates can be obtained by correcting the pitch curve coordinates taking into account a roller radius greater than zero.

$$h_{CAM\,real} = \sqrt{(l_{RC}\sin\beta - R_r\sin\phi)^2 + (l_{PC} - l_{RC}\cos\beta - R_r\cos\phi)^2} \quad (30)$$

$$\delta_{real} = \theta_P + \tan^{-1}\frac{l_{RC}\sin\beta - R_r\sin\phi}{l_{PC} - l_{RC}\cos\beta - R_r\cos\phi} \quad (31)$$

where Rr = 18 mm is the roller radius and ϕ can be obtained through Eq.(18). The smoothed cam profile is shown in Figure 30 compared to the smoothed pitch curve.

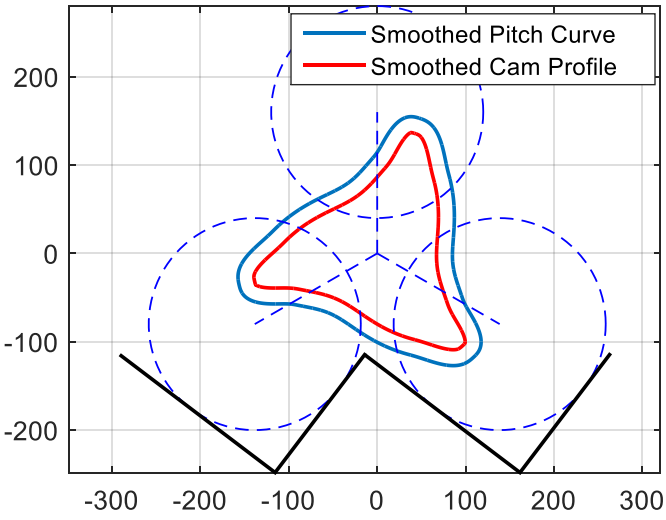

Figure 30 - Comparison between the smoothed pitch curve and the smoothed cam profiles

In Figure 31 the radius of curvature and the pressure angle of the smoothed cam profile are presented. The selected roller radius (Rr = 18mm) is near to the maximum admissible value to avoid undercutting and thus is yet at the correct value. As regard pressure angle, its maximum value is increased with respect to the unsmoothed profile due to the local growth of the derivative of $\alpha^*(\theta_P)$ compared to the derivative of $\alpha(\theta_P)$. The maximum pressure angle is a bit higher than 50°, that can be considered as an upper limit. In order to reduce the maximum value for pressure angle, all the algorithm described in this paragraph should be repeated starting from a higher dimension for the cam. In other words, the design procedure should be repeated using a parameter D greater than 1 that was the value used for the first iteration.

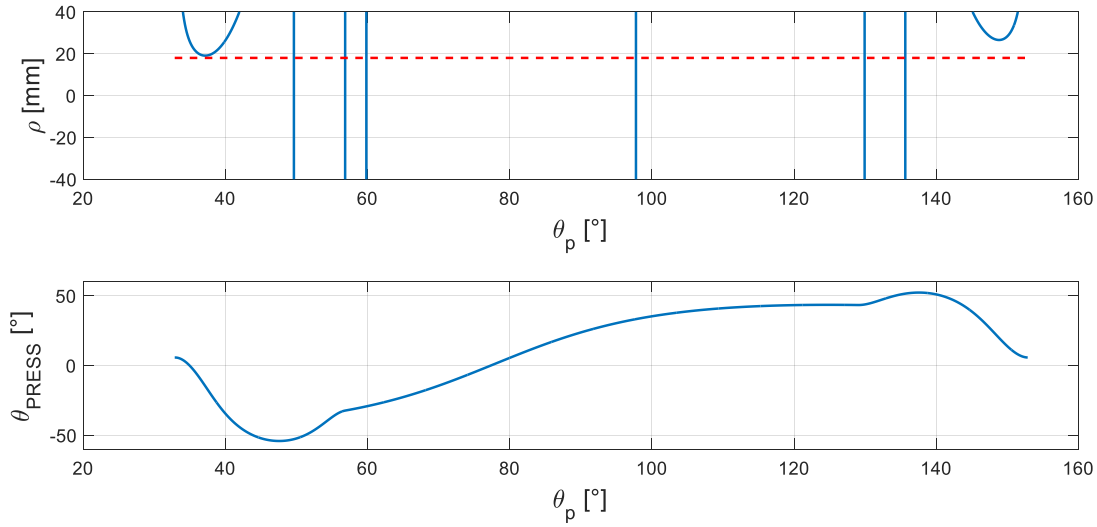

Figure 31 – Trend of radius of curvature and pressure angle for the smoothed cam profile (the red dashed line represents the dimension of the roller radius)

A final analysis has been conducted in order to assess the influence of parameter D over the $\max(|\theta_{PRESS}|)$ value of the smoothed cam profile. This analysis is necessary in order to identify the proper value for D with which repeat the cam synthesis algorithm. The maximum pressure angle decreases with the increase of the cam dimension as can be observed in Figure 32. In order to obtain a maximum pressure angle equal to 50° it is necessary to impose a dimensionless size of the cam D = 1.135.

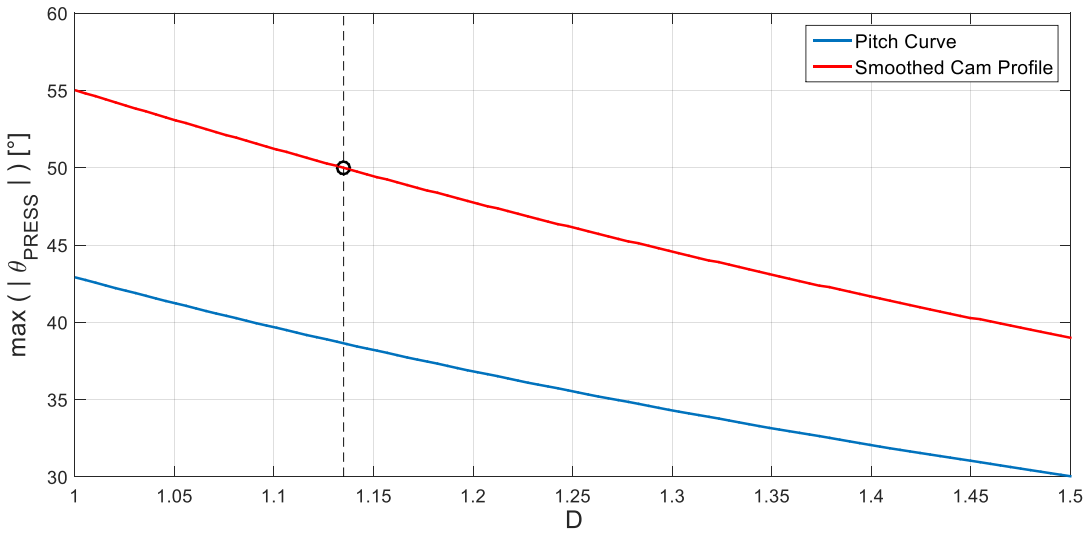

Figure 32 – Trend of max(|θ_{PRESS}|) *with respect to D for pitch curve and smoothed cam profile*

With this value of D, the procedure explained in this section can be repeated. The smoothed cam profile obtained with the most favorable values for I, R and β_0 it is showed in Figure 33 and the mechanism parameters are summarized in Tab.4 in comparison with the parameters obtained from the previous iteration. It can be observed that the cam dimension is adequate to avoid interferences with step edges and so this profile can be considered verified under all the design requirements. In Figure 34 a step climbing sequence with the best cam mechanism is presented.

Table 4 -Comparison between the best mechanism parameters for the profile obtained after the first iteration and after the complete design process

Parameter	**D**	**l_{PC}**	**R**	**l_{RC}**	**β_0**	**max(|θ_{PRESS}|) pitch curve**	**max(|θ_{PRESS}|) smoothed cam profile**	**I**
		[mm]		[mm]	[°]	[°]	[°]	
First iteration values	1	800	0.96	768	11.5	43.0	54.14	5
Final values	1.13	800	0.95	760	13.1	38.64	50	5

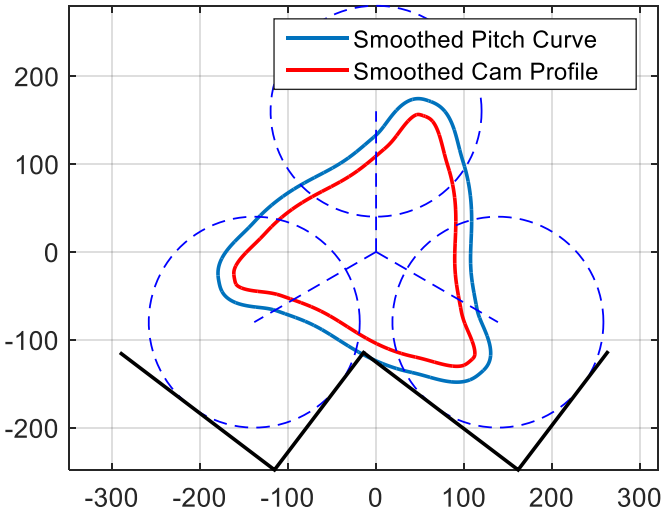

Figure 33 – Comparison between smoothed pitch curve and smoothed cam profile with the best mechanism parameters

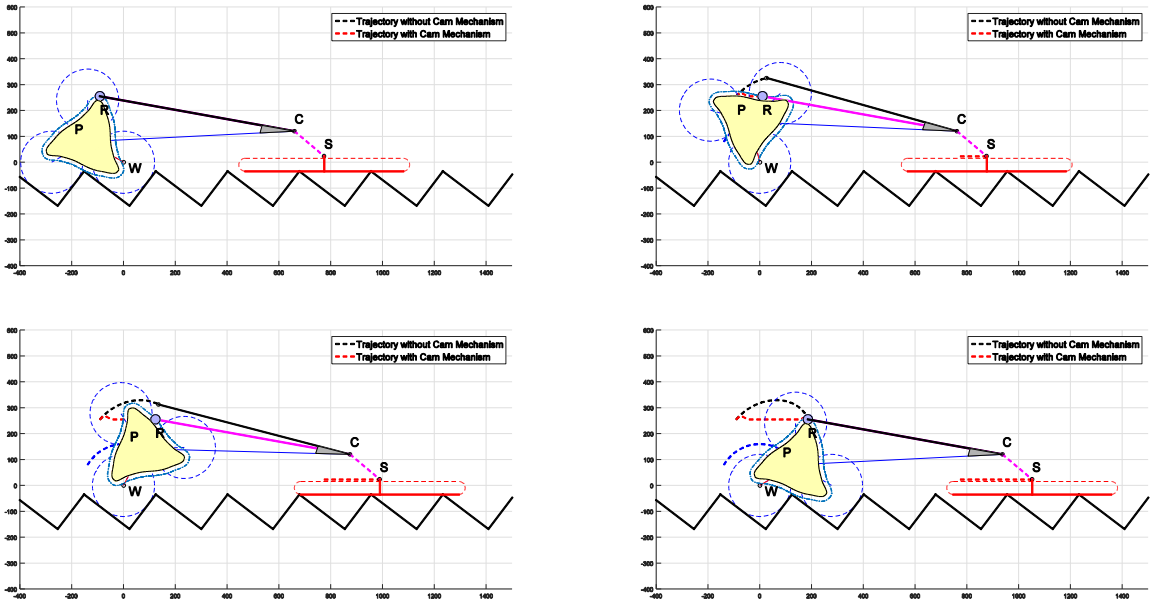

Figure 34 – Step climbing sequence with the best cam mechanism

5. Conclusion

In this paper, a new version of the stair-climbing device *Wheelchair.q* has been proposed. This new concept tries to overcome the unsolved problems related to previous versions through a different wheelchair architecture. The main idea was to define a smart mechanical structure, able to reduce as much as possible the number of the actuators and mechatronic subsystems, in order to guarantee lightweight, safety, comfort, and reduced costs. The idle track that represents the rear foothold for the wheelchair during stair-climbing is moved to the rear with respect to previous versions. This innovation allows to increase the static stability and to reduce the seat oscillation during stair-climbing activity. In particular, the reduction of the seat oscillation has been the focus of this new design. A cam mechanism with a swinging follower has been added to the wheelchair structure with the aim to passively compensate the oscillation introduced on the device frame by the locomotion unit rotation. Thanks to the cam mechanism action, the wheelchair seat moves with a translational motion along a straight line, increasing the user comfort. The main topic of this paper has

been the description of the design process that has brought to the choice of a proper cam profile. In the first part, the locomotion unit motion has been described and the algorithm necessary to obtain the cam profile has been presented. In the second part, a parametric analysis on the mechanism has been conducted. The results have been used to choose the most favorable parameters in order to have the smallest cam with acceptable values for pressure angle and curvature radius.

Future works will regard the design and optimization of the other parts of the wheelchair structure that are not already completely defined. In particular, the reconfiguration mechanism that should modify the wheelchair configuration before stair-climbing must be analyzed.

Once the design process will be completed, a multibody analysis of the vehicle should be conducted in order to finalize the design process before starting with an experimental activity on a prototype.

References

[1] Papworth Trust, “Disability in the United Kingdom 2014: Facts and Figures”, 2014

[2] U.S Census Bureau, “Americans with Disabilities: 2005”, 2008

[3] Disability Statistics Center Institute for Health and Aging, University of California, “Mobility Device Use in the United States”, 2000

[4] L. Bruzzone, G. Quaglia, "Review article: locomotion systems for ground mobile robots in unstructured environments", Mechanical Sciences, Vol. 3, 2012, pp. 49-62.

[5] Y. Sugahara et al., "Walking up and down stairs carrying a human by a biped locomotor with parallel mechanism", Proceeding of International Conference on Intelligent Robots and Systems (IROS), 2005, Edmonton, Alberta, Canada, pp.1489-1494.

[6] S. Yu, T. Wang et al., "A tip-over and slippage stability criterion for stair-climbing of a wheelchair robot with variable geometry single tracked mechanism", Proceeding of International Conference on Information and Automation (ICIA), 2012, Shenyang, China, pp.88-93.

[7] S. Yu, T. Wang et al., "Configuration and tip-over stability analysis for stair-climbing of a new-style wheelchair robot", Proceeding of International Conference on Mechatronics and Automation (ICMA), 2010, Xi'an, China, pp.1387-1392.

[8] H. Wang, W. Zhang et al., "Research on a kind of leg-wheel stair-climbing wheelchair", Proceeding of International Conference on Mechatronics and Automation (ICMA), 2014, pp.2101-2105.

[9] Y. Bang, C. Lee et al., "Two-legged stair-climbing wheelchair and its stair dimension measurement using distance sensors", Proceeding of International Conference on Control, Automation and Systems (ICCAS), 2011, Gyeonggi-do, Korea, pp.1788-1791.

[10] J. Yuan, S. Hirose, "Research on leg-wheel hybrid stair-climbing robot, Zero Carrier", Proceeding of International Conference on Robotics and Biomimetics (ROBIO), 2004, Shenyang, China, pp.654-659.

[11] M. J. Lawn, T. Ishimatsu, "Modeling of a stair-climbing wheelchair mechanism with high single-step capability", Neural Systems and Rehabilitation Engineering, Vol. 11, No. 3, 2003, pp.323-332.

[12] J. Liu, Y. Wu et al., "High-Order Sliding Mode-Based Synchronous Control of a Novel Stair-Climbing Wheelchair Robot", Journal of Control Science and Engineering, 2015.

[13] A. Gonzalez, R. Morales et al, "Improving the mechanical design of new staircase wheelchair", Industrial Robot: An International Journal, Vol. 34, No. 2, 2007, pp.110-115.

[14] A. Gonzalez, E. Ottaviano, M. Ceccarelli, "On the kinematic functionality of a four-bar based mechanism for guiding wheels in climbing steps and obstacles", Mechanism and Machine Theory, Vol. 44, No.8, 2009, pp.1507-1523.

[15] J. Chocoteco, R. Morales, V. Feliu, "Improving the climbing/descent performance of stair-climbing mobility systems confronting architectural barriers with geometric disturbances", Mechatronics, Vol. 30, 2015, pp.11-26.
[16] R. Morales, V. Feliu et al., "Coordinated motion of a new staircase climbing wheelchair with increased passenger comfort", Proceeding of International Conference on Robotics and Automation (ICRA), 2006, Orlando, Florida, USA, pp.3995-4001.
[17] R. Morales, V. Feliu and A. González, "Optimized obstacle avoidance trajectory generation for a reconfigurable staircase climbing wheelchair", Robotics and Autonomous Systems, Vol. 58, No.1, 2010, pp.97-114.
[18] S. Motoki, N. Tomokuni et al., "Wheeled inverted pendulum type robotic wheelchair with integrated control of seat slider and rotary link between wheels for climbing stairs", Workshop on Advanced Robotics and its Social Impacts (ARSO), 2014, Evanston, Illinois, USA, pp.121-126.
[19] N. M. A. Ghani, A. N. K. Nasir, M. O. Tokhi, "Optimization of fuzzy logic scaling parameters with spiral dynamic algorithm in controlling a stair climbing wheelchair: Ascending task", Proceeding of International Conference on Methods and Models in Automation and Robotics (MMAR), 2014, Międzyzdroje, Poland, pp. 776-781.
[20] C. Chen, H. Pham, "Design and fabrication of a statically stable stair-climbing robotic wheelchair", Industrial Robot: An International Journal, Vol. 36, No.6, 2009, pp.562-569.
[21] Y. Sugahara, N. Yonezawa, K. Kosuge, "A novel stair-climbing wheelchair with transformable wheeled four-bar linkages", Proceeding of International Conference on Intelligent Robots and Systems (IROS), 2010, Taipei, Taiwan, pp.3333-3339.
[22] Kenneth Ray Cox, "Battery powered stair-climbing wheelchair", U.S. Patent No. 6484829, Nov. 26, 2002.
[23] G. Quaglia et al., "The Epi. q-1 hybrid mobile robot", The International Journal of Robotics Research, Vol.29, No.1, 2009, pp. 81-91.
[24] G. Quaglia, L. Bruzzone et al., "A modular approach for a family of ground mobile robots", International Journal of Advanced Robotic Systems, Vol.10, 2013.
[25] G. Quaglia, M. Nisi, “Design and construction of a new version of the Epi.q UGV for monitoring and surveillance tasks”, Proceeding of the International Mechanical Engineering Congress & Exposition (IMECE), 2015, Houston, Texas.
[26] G. Quaglia, W. Franco, R. Oderio, "Wheelchair. q, a motorized wheelchair with stair climbing ability", Mechanism and Machine Theory, Vol.46, No.11, 2011, pp.1601-1609.
[27] G. Quaglia, W. Franco, R. Oderio, "Wheelchair. q, a mechanical concept for a stair climbing wheelchair", Proceeding of International Conference on Robotics and Biomimetics (ROBIO), 2009, Guilin, China, pp.800-805.
[28] G. Quaglia, W. Franco, M. Nisi, "Design of a Reconfiguration Mechanism for an electric Stair-climbing Wheelchair", Proceeding of the International Mechanical Engineering Congress & Exposition (IMECE), 2014, Montreal, Quebec, Canada.
[29] G. Quaglia, W. Franco, M. Nisi, "Evolution of Wheelchair. q, a Stair-climbing Wheelchair", Proceeding of the 14th World Congress in Mechanism and Machine Science, 2015, Taipei, Taiwan.
[30] R. L. Norton, “Design of machinery: an introduction to the synthesis and analysis of mechanisms and machines”, McGraw-Hill Professional, 2004.
[31] P. L. Magnani, G. Ruggieri, “Meccanismi per macchine automatiche”, Utet, 1986.